Identification and Modeling of Driver Multiloop Feedback and Preview Steering Control

van der El, Kasper; Pool, Daan; van Paassen, Rene; Mulder, Max

DOI
10.1109/SMC.2018.00215

Publication date
2018

Document Version
Accepted author manuscript

Published in
Proceedings of the IEEE International Conference on Systems, Man, and Cybernetics

Identification and Modeling of Driver Multiloop Feedback and Preview Steering Control

Kasper van der El, Daan M. Pool, Marinus (René) M. van Paassen, and Max Mulder
Control & Simulation section, Faculty of Aerospace Engineering
Delft University of Technology, Delft, The Netherlands
Email (corresponding author): k.vanderel@tudelft.nl

***Abstract*—Novel (semi-)automated systems are rapidly being introduced into modern road vehicles, but anticipating possibly critical human-machine interaction issues is difficult, because the human driver's behavior is as of yet still poorly understood. This paper aims to improve our understanding and models of driver steering behavior on winding roads, using Frequency-Response Function (FRF) measurements of drivers' feedforward, heading feedback, and lateral position feedback dynamics. The steering behavior data were collected in a human-in-the-loop simulator experiment, in which drivers followed the road centerline at constant forward velocity, while being perturbed laterally by wind-gust disturbances. All three measured FRFs can be captured with a multiloop, single preview-point driver model, which has only five parameters. These parameters provide unmatched understanding of – otherwise lumped – driver internal steering processes, quantifying how and what portion of the previewed centerline trajectory is used for control, and how lateral position and heading feedback are weighed. The gained insights may help to reduce driver-automation interaction issues in modern road vehicles, to quantify between-driver steering variations, adaptation and learning, and to design human-like and individualized automatic and shared steering controllers.**

I. Introduction

Road vehicles are rapidly being equipped with more Advanced Driver Assistance Systems (ADAS) and even autopilots for (temporary) autonomous control. It is difficult to anticipate how human drivers of such vehicles, as well as other road users, will interact with the novel automation systems. To better understand potential human-machine interaction issues in tomorrow's vehicles, a profound understanding of *human* driver behavior is desirable.

Considering the task of *steering*, drivers are known to rely heavily on visual feedback [1]. It has been suggested that drivers use patterns of the optical flow for control [2]–[5], "near" and "far" regions in the visual field [6], [7], and the road's curvature or tangent point [8]. Moreover, control-theory has shown that drivers combine *feedforward* control to follow the road's curves, with *feedback* control to stabilize the vehicle [9]–[13]. Nonetheless, neither driver feedforward nor feedback steering behavior are as of yet fully understood, and not due to a lack of testable theories or models [12], [13]. Feedforward steering behavior has been modeled using either one, two, or many points of the previewed trajectory as input (e.g., see [9], [10], [14]–[16]). Driver feedback behavior, besides indispensable lateral-position outer-loop control, has been modeled either as a linear or model-based prediction process, or as an inner-loop based on vehicle heading or path angle [17], [18].

In order to better understand driver steering, and favor one model or theory over another, we need measurements of the driver's *control dynamics*, such as Frequency-Response Function (FRF) data [19]. McRuer *et al*. [20] based their seminal *crossover model* for single-loop compensatory tracking tasks on FRF measurements. McRuer and his colleagues [9], [18] have in fact extended the original crossover model with a heading-angle inner-loop response to capture driver FRF data for the task of suppressing (wind-gust) disturbances on straight roads. More recently, *multiloop* FRF estimates proved indispensable for understanding and modeling the human's feedforward and feedback control responses in tracking tasks with preview [21], [22].

This paper aims to improve our understanding and models of driver steering behavior on winding roads using similar FRF measurements. Steering data were gathered in a human-in-the-loop simulator driving experiment, in which subjects tracked the road's centerline (to limit variability in behavior), while simultaneously suppressing wind-gust disturbances. For the first time, the dynamics of *three* driver responses are estimated, namely their feedforward, or *preview* response, as well as their *heading* and *lateral position* feedback responses. Moreover, we propose a novel driver steering model that combines well-validated, existing models for compensatory tracking (the crossover model [20]), straight road driving [18], and single-loop preview tracking tasks [21], [22]. We will show that the proposed multiloop model does not only capture all three estimated driver FRFs *and* the driver's steering output, but additionally does so with *physically interpretable* model parameters.

II. Control-Theory of Driver Steering

A. Control Task

The considered driving task is illustrated in Fig. 1. The driver is to track the road's centerline (i.e., the target trajectory y_c), while simultaneously suppressing wind-gust disturbances (y_d laterally and ψ_d on heading). The driver thus effectively minimizes the lateral position error $y_e = y_c - y$, with y the vehicle's lateral position. To do so, drivers rotate the steering wheel (angle δ), based on perceived optical cues visible through the vehicle's front windshield.

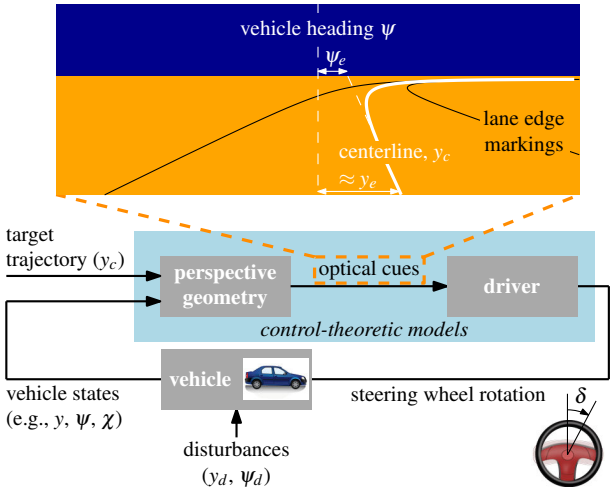

Fig. 1. Schematic of the driver in a steering task. Control-theoretic models typically lump the perspective geometry and driver blocks, ignoring driver optical cue selection.

B. Control-Theoretic Driver Model

1) Single-Loop Compensatory Tracking: Fig. 2 shows the proposed quasi-linear model for driving along winding roads. The model's central element, or inner loop, is equivalent to the *simplified precision* model for the human's compensatory error response H_o^{comp} [20]. This model contains an equalization gain $K_{e^\star}$, equalization lead time-constant $T_{L,e^\star}$, and response time delay $\tau_{e^\star}$. An additional model for the driver's neuromuscular activation dynamics is sometimes included in H_o^{comp} [20], [21], but is left out here for simplicity.

2) Straight Road Driving: In driving tasks more than one feedback variable is generally available, yielding a *multiloop* control task. Drivers most likely use the vehicle's heading as input to the compensatory inner-loop [9], [18], as shown in Fig. 2. Nonetheless, other quantities such as the vehicle's path angle also yield satisfactorily inner-loop characteristics [17], and could be used (intermittently) by human drivers. The inner-loop closure provides the lead equalization required to obtain a stable integrator magnitude slope around the open-loop crossover frequency [11], [17], [20]. Consequently, drivers can close the lateral position outer-loop using proportional control, see Fig. 2; the gain K_y^ψ characterizes drivers' relative weighing of heading and lateral position feedback.

3) Preview Processing: Human use of preview information was modeled with a pre-filter $H_{o_f}(j\omega)$ that outputs a single processed target position $y_c^\star(t)$ [21], [22], see Fig. 2. τ_f is the farthest point ahead on the target trajectory that is used by the human for control and $T_{l,f}$ is the time constant of the low-pass smoothing filter. Due to the low-pass filter, the processed trajectory is identical to the original trajectory at low frequencies, but attenuated at high frequencies, such that the road's tighter corners are cut. The human's level of pursuit control is characterized by gain K_f; $K_f < 1$ indicates that drivers prioritize vehicle stabilization (feedback) over tracking of the target trajectory (feedforward) [22]. When K_f=1 m/m and τ_f=$T_{l,f}$=0 s, the processed target $y_c^\star$ equals the actual lateral position of the road's centerline and the model reduces to the model for straight road driving, see Fig. 2.

III. System Identification

To measure the driver's multiloop response dynamics, we apply two distinct system identification techniques. First, three FRFs are estimated to obtain nonparametric estimates of the driver's multiloop control dynamics. Second, the proposed multiloop driver model is fit to the data, yielding estimates of the model parameters. The model is validated by comparing both the modeled and measured steering output, and the modeled and measured (FRFs) control dynamics in Bode plots.

A. Parallel Three-Channel Model Structure

To measure FRFs of the driver's heading feedback, lateral position feedback, and target feedforward response dynamics, $H_{o_\psi}(j\omega)$, $H_{o_y}(j\omega)$, and $H_{o_{y_c}}(j\omega)$, respectively, we adopt the parallel model structure in Fig. 3. We do *not* imply that drivers are internally organized as such; this structure is only used as a convenient tool for measuring driver multiloop steering dynamics. As indicated by the corresponding yellow, green, and pink blocks in Figs. 2 and 3, the estimated FRF dynamics are related to the proposed multiloop model as follows:

$$H_{o_\psi}(j\omega) = H_o^{comp}(j\omega), \tag{1}$$

$$H_{o_y}(j\omega) = K_y^\psi H_o^{comp}(j\omega), \tag{2}$$

$$H_{o_{y_c}}(j\omega) = H_{o_f}(j\omega) K_y^\psi H_o^{comp}(j\omega). \tag{3}$$

For example, an FRF estimate of the H_{o_y} block with flat magnitude would reflect gain dynamics, or a driver response proportional to lateral position y; alternatively, differentiator dynamics would indicate a response to $\dot{y}$, or the vehicle path angle. Note that the H_{o_ψ} block drops from the model in single-loop display tracking tasks (e.g., [20], [21]), or when drivers fail to mechanize an inner loop, for example due to a lack of rotational cues while driving in dense fog. Equivalently, the $H_{o_{y_c}}$ block disappears in compensatory, straight road driving tasks (i.e., $y_c = 0$).

B. Road Trajectory and Wind-Gust Disturbances

FRFs of the $H_{o_{y_c}}$, H_{o_y}, and H_{o_ψ} blocks can be obtained only when the three external external excitation signals, y_c, y_d, and ψ_d, Fig. 3 are uncorrelated [23]. Common practice in manual control experiments is to use random-appearing multisine signals [18], [19], [21]–[24]. Here, we design the road's trajectory to be the sum of 10 sinusoids: $y_c(a) = \sum_{i=1}^{10} A[i]\sin(\omega[i]a + \phi[i])$, with amplitude $A[i]$, frequency $\omega[i]$, and phase $\phi[i]$ of the i-th sinusoid, and a the along-track distance [14]. The heading and lateral position disturbances are defined identically, see Table I for their parameters. Mutually exclusive input frequencies ω_{y_c}, ω_{ψ_d}, and ω_{y_d} are selected such that the three forcing functions are uncorrelated. All frequencies $\omega[i]$ are integer multiples k of the fundamental frequency ($\frac{2\pi}{1389} = 0.0045$ rad/m) that corresponds to the 1389 m long measurement part of the track. A reasonably low-frequency driving task was obtained by attenuating the

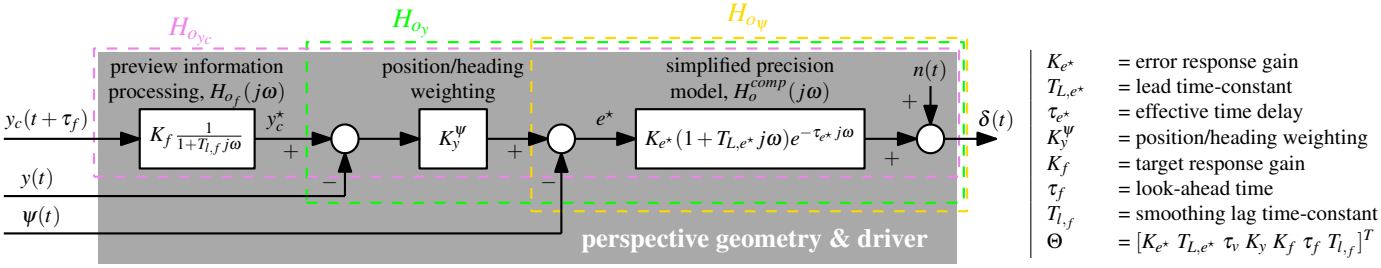

Fig. 2. Control-theoretic model for driver steering on winding roads, obtained by combining the multiloop compensatory driver model for (wind-gust) disturbance-rejection on straight roads [18], and the model for preview processing in single-loop display tracking tasks [21]. The model is a lumped combination of the driver and perspective geometry blocks in Fig. 1. The colored portions of the model correspond to Fig. 3.

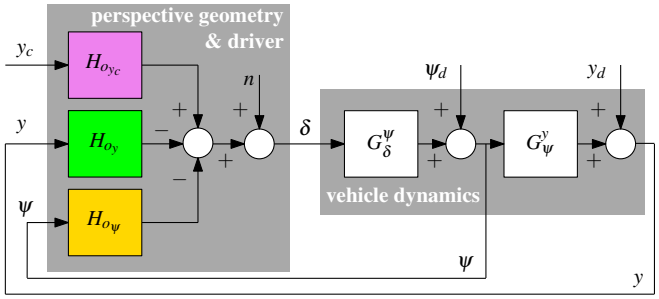

Fig. 3. Three-channel parallel control diagram used for measuring FRFs of drivers' multiloop steering dynamics; colored blocks correspond to Fig. 2.

amplitudes $A[i]$ at higher frequencies, see Table I. The phases $\phi[i]$ were randomized in accordance with the method in [24]. Five different phase realizations were used for y_c to prevent subjects from memorizing parts of the road's trajectory.

C. System Identification Techniques

Exploiting the uncorrelated external signals as instrumental variables, FRF measurements of $H_{o_{yc}}(j\omega)$, $H_{o_\psi}(j\omega)$, and $H_{o_y}(j\omega)$ can be obtained directly at the multisine input frequencies ω_{y_c}, ω_{ψ_d} and ω_{y_d}, see [22], [23] for details. An estimate of the proposed model's parameter vector $\hat{\Theta}$ (see Fig. 2) is obtained by minimizing the least-squares error between the measured (δ) and modeled ($\hat{\delta}$) steering wheel rotations in the frequency-domain, with $\hat{\delta}(j\omega) = H_{o_{yc}}(j\omega)Y_c(j\omega) - H_{o_\psi}(j\omega)\psi(j\omega) - H_{o_y}(j\omega)Y(j\omega)$, see Fig. 3. The Variance Accounted For (VAF) is used as measure for the model quality-of-fit [22]; the maximum VAF is 100% and reflects a model that perfectly replicates the measured control output.

IV. Driving Experiment

A. Independent Variables

The experiment had two independent variables. First, driving on straight (y_c=0) and winding roads ($y_c \neq 0$) was compared, yielding a compensatory (C) disturbance-rejection task, and a pursuit (P) task that combines target-tracking with disturbance-rejection, respectively. Second, both tasks were performed both with a fixed (F) viewing direction, in which the vehicle does not rotate but moves only laterally, and with a naturally rotating (R) view that is always aligned with the vehicle's heading ψ. The fixed viewing direction provides subjects with information of vehicle lateral position and path, but lacks heading cues. These fixed-view tasks are identical to the well-understood, *single-loop* compensatory [20] and preview display tracking tasks [22]. The rotating view additionally conveys heading information, identical to normal driving tasks. The full factorial of the two independent variables was tested, yielding four experimental conditions, abbreviated as CF, CR, PF, and PR.

Fig. 4. The SIMONA research simulator, outside and inside.

B. Apparatus

The experiment was performed in the SIMONA Research Simulator (SRS) at TU Delft, Fig. 4, of which the left side was equipped with a customized passenger-car steering wheel. Visuals were presented on the simulator's collimated projection system, which provided subjects with a 180×40 deg field of view, see Fig. 4. The vehicle moved at constant forward velocity (U_0 =13.89 m/s =50 km/h), and the inner-(ψ) and outer-loop (y) vehicle dynamics, G_δ^ψ and G_ψ^y, Fig. 3, are approximated as pure integrators, identical as in [10]. The steering wheel gain was set to 1.33 (deg/s)/deg.

TABLE I
AMPLITUDES, FREQUENCIES AND INITIAL PHASES OF THE TARGET AND DISTURBANCE FORCING FUNCTION SIGNALS.

	road center-line, y_c RMS(y_c) = 13.1 m, RMS(ψ_c) = 15 deg								disturbance, y_d RMS(y_d) = 0.3 m, RMS(β) = 1.27 deg				disturbance, ψ_d RMS(ψ_d) = 2.2 deg			
i -	k -	ω rad/m	A m	ϕ_1 rad	ϕ_2 rad	ϕ_3 rad	ϕ_4 rad	ϕ_5 rad	k -	ω rad/m	A m	ϕ rad	k -	ω rad/m	A deg	ϕ rad
1	3	0.01	17.70	2.92	5.05	4.00	2.66	0.80	5	0.02	0.29	5.98	7	0.03	2.20	5.04
2	9	0.04	5.02	1.49	2.99	5.12	2.71	1.08	11	0.05	0.24	4.04	13	0.06	1.74	6.22
3	15	0.07	2.33	4.85	5.23	3.73	1.36	0.53	19	0.09	0.16	3.05	23	0.10	1.08	4.17
4	27	0.12	0.73	4.26	2.98	0.17	4.08	3.88	31	0.14	0.09	6.11	35	0.16	0.63	4.40
5	39	0.18	0.30	6.20	5.00	2.02	5.10	2.74	43	0.19	0.06	0.99	47	0.21	0.41	4.97
6	53	0.24	0.14	1.61	2.11	2.51	2.98	3.93	59	0.27	0.04	0.01	65	0.29	0.25	4.97
7	71	0.32	0.07	0.83	0.32	3.93	4.92	3.58	77	0.35	0.02	1.78	85	0.38	0.16	4.10
8	93	0.42	0.03	1.31	1.03	1.49	5.97	5.21	101	0.46	0.02	2.28	111	0.50	0.11	5.90
9	121	0.55	0.02	0.35	4.45	5.88	3.08	4.14	131	0.59	0.01	0.41	143	0.65	0.08	5.48
10	155	0.70	0.01	4.21	5.96	0.62	5.75	5.69	169	0.76	0.01	2.41	183	0.83	0.07	0.73

C. Participants, Instructions, and Procedures

Eight motivated volunteers participated in the experiment, all students or staff from TU Delft. All subjects signed for informed consent prior to the experiment, and were instructed to follow the displayed centerline as accurately as possible.

Subjects were seated on the left side of the simulator, with fastened seat belt. First, a single run of each condition was performed to familiarize subjects with the steering wheel, the vehicle dynamics, and the display. Then, the four experimental conditions were performed in an order randomized according to a balanced Latin-square design. A condition was performed at least until tracking performance (RMS(y_e)) and control activity (RMS(δ)) were approximately constant in five consecutive runs, which were then used for further analysis. A single run was 1806 m, but included 278 m run-in and 139 m run-out; only the steering data in the remaining 1389 m measurement portion of the track were used for analysis. During the experiment, time traces of the applied steering wheel rotations δ and vehicle lateral position y and heading ψ were recorded at 100 Hz.

V. RESULTS

A. Multiloop FRF Estimates

1) Heading Response: The heading FRF $H_{o_\psi}(j\omega)$ (red markers in Fig. 5), estimated from experimental data in the rotating-view PR task, is a relatively smooth function of frequency, and variations between the five measurement runs are small (i.e., reasonably small errorbars). In contrast, the estimated FRF components in the fixed-view PF task (blue markers) have a much lower magnitude and considerable variation between runs, while the estimated phases are an inconsistent function of frequency. The FRF estimates in the fixed-view tasks in general appear to reflect pure noise and therefore suggest that no consistent heading response was active, whereas the FRF estimates in rotating-view tasks provide strong evidence that subjects indeed consistently used heading feedback for controlling their vehicle.

2) Multiloop Feedback Dynamics: Fig. 5 shows that $H_{o_y}(j\omega)$ in fixed-view tasks (PF, blue markers) approximates gain dynamics at low frequencies, and differentiator dynamics at high frequencies, with notable phase lead for frequencies up to 4 rad/s. This indicates responses proportional to the vehicle's lateral position and velocity (i.e., path angle). Thereby, the double-integrator lateral position vehicle dynamics are equalized to an integrator open-loop in the crossover region, yielding a stable system even without a heading-loop closure. In rotating-view tasks (PR, red markers), the required stabilizing lead is instead obtained from the heading-loop closure. Both $H_{o_\psi}(j\omega)$ and $H_{o_y}(j\omega)$ approximate gain dynamics up to frequencies well beyond crossover, indicating inner- and outer-loop responses proportional to the vehicle's heading angle and lateral position, respectively. The slight increase in magnitude at the highest frequencies may indicate lead, that is, relatively weak responses proportional to path angle and heading rate, or oscillatory behavior due to drivers' neuromuscular system dynamics.

3) Feedforward Dynamics: In both fixed- and rotating-view tasks, the magnitude of the feedforward response FRF approximates gain dynamics, see Fig. 5. This suggests that subjects responded to the lateral position of the centerline, and not its heading or curvature. Increasing phase lead is visible at higher frequencies, corresponding to the behavior of a negative time delay, or a *look-ahead time* (i.e., τ_f in Fig. 2) [21]. The FRF estimates of $H_{o_{y_c}}(j\omega)$ are relatively noisy at the very highest frequencies, because the available preview allows subjects to recognize and ignored much of these fast oscillations of the centerline trajectory, leading to a low signal-to-noise ratio (not shown).

B. Model Fits

1) Quality-of-Fit: The model matches the measured steering wheel angles δ well in all four conditions, as indicated by an average VAF over the eight subjects above 90% (Table II). Moreover, besides capturing the driver's *output*, Fig. 5 shows that the proposed model also captures the driver's *multiloop*

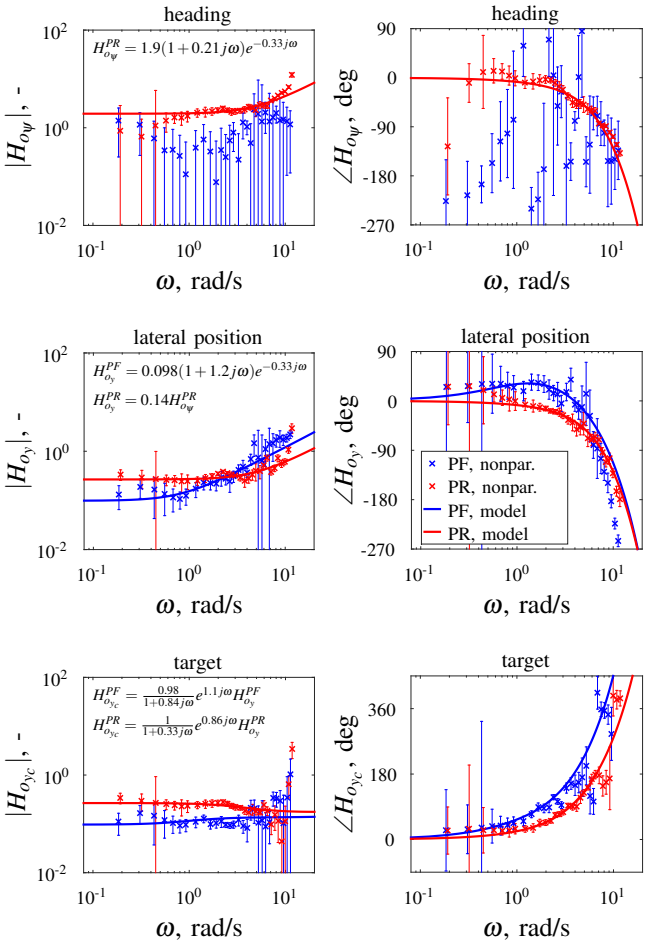

Fig. 5. Bode plots of estimated multiloop response dynamics in winding road conditions: nonparametric FRF estimates and model fits for Subject 1. The model fit in the fixed-view (PF) task was obtained with a reduced model that lacks the $H_{o_\psi}(j\omega)$ response, as the FRF estimates indicate that no consistent heading response was active. Estimates of $H_{o_y}(j\omega)$ and $H_{o_\psi}(j\omega)$ are equivalent in straight road tasks (not shown).

control dynamics. The shape of the FRF estimates of the driver's lateral position feedback, heading feedback, and feedforward response dynamics are *all* captured by the model. Only at the very lowest and highest input frequencies there is a small discrepancy between the model and the FRFs, because several FRF components are poorly estimated (large errorbars) and because no element for the driver's neuromuscular system dynamics was included in the model.

2) Parameter Estimates: Subjects strongly adapt their equalization dynamics between tasks, see $K_{e^\star}$ and $T_{L,e^\star}$ in Table II. Tasks with viewing rotations (CR and PR), where equalizing lead is obtained from the heading-loop closure, evoke markedly less explicit lead equalization (lower $T_{L,e^\star}$), but a substantially higher control gain $K_{e^\star}$ as compared to fixed-view tasks (CF and PF). Similarly, $T_{L,e^\star}$ decreased while $K_{e^\star}$ increases from straight to winding road tasks. The response delay $\tau_{e^\star}$ is slightly higher in rotating-view tasks, Table II. A similar increase in visual response delay has been observed

TABLE II
ESTIMATED MODEL PARAMETERS, AVERAGE OVER EIGHT SUBJECTS AND STANDARD DEVIATIONS.

	straight CF	straight CR	curved PF	curved PR
VAF, %	92.3±3.33	94.6±1.24	91.2±1.91	94.2±1.10
$K_{e^\star}$, rad/rad	0.11±0.03	1.19±0.40	0.14±0.02	2.06±0.18
$T_{L,e^\star}$, s	1.44±0.40	0.40±0.12	0.90±0.13	0.19±0.02
$\tau_{e^\star}$, s	0.33±0.03	0.35±0.02	0.30±0.02	0.34±0.02
K_y^ψ, rad/m	-	0.18±0.04	-	0.12±0.01
K_f, m/m	-	-	0.99±0.01	1.00±0.00
$T_{l,f}$, s	-	-	0.86±0.07	0.26±0.13
τ_f, s	-	-	1.06±0.05	0.89±0.11

when motion feedback is made available in compensatory tracking tasks [25]; likely, there is no incentive for subjects to put effort into reducing their delay due to the increased stability provided by the additional heading loop closure.

Subjects' relative weighting of lateral position and heading feedback, K_y^ψ, is slightly higher on straight roads as compared to winding roads, see Table II. This indicates that subjects minimize lateral position errors more aggressively. The target weighting gain K_f approximates unity, both in tasks with and without viewing rotations, such that K_f could in fact be dropped from the proposed model. The farthest point on the previewed trajectory used for control, characterized by τ_f, is approximately 1.1 s in fixed-view tasks, which matches well with measurements in preview tracking experiments [22]. τ_f is slightly lower in rotating-view tasks, around 0.9 s, which is partly because a shorter portion of the previewed trajectory is used for smoothing (lower $T_{l,f}$). The lower $T_{l,f}$ in rotating-view tasks further suggests that subjects cut less corners and follow more of the centerline's higher frequencies.

VI. Discussion

The proposed multiloop model does not only capture drivers' steering *output* well (high VAFs), but it is the first driver model that has been shown to also match drivers' *multiloop control dynamics* (feedforward on the previewed target, and vehicle heading and lateral position feedback). In addition, the model directly extends McRuer's seminal crossover model [20], the most widely accepted and applied model of manual control to date. After dropping K_f, which was identified to be unity, the multiloop model can describe driver steering with only six parameters. Each of these parameters has a direct physical interpretation in terms of drivers' compensatory control behavior ($K_{e^\star}$, $T_{L,e^\star}$, $\tau_{e^\star}$), their use of preview information (τ_f, $T_{l,f}$), and their relative priority for heading or lateral position feedback (K_y^ψ). Moreover, McRuer and his colleagues [17], [18] have explained how K_y^ψ can be interpreted as a look-ahead time, given by $\frac{1}{U_0 K_y^\psi}$. This look-ahead time is on average 0.62 s (SD = 0.08) for our eight subjects in the full driving task (PR). Compensating τ_f for the phase lag introduced by the low-pass smoothing filter, $\tau_f - T_{l,f}$, surprisingly yields almost the same result, namely 0.63 s (SD = 0.08). This suggests that drivers base

their feedback and feedforward control behavior on optical cues that are located approximately equally far ahead of the vehicle in the visual scene. We aim to further investigate the physical interpretation and the implications of this striking observation in our future work. Tentatively, driver behavior may thus even be captured with only *five* model parameters, without sacrificing any of our model's descriptive ability.

The measured feedforward FRF ($H_{o_{y_c}}$) could be captured well with our *single* preview-point driver model. This strongly suggests that drivers do *not* mechanize a second response based on a different point along the previewed centerline trajectory, as opposed to human controllers in single-loop preview tracking tasks [21], [22]. The implications of this result are profound, suggesting that previously proposed, more complex two-point [15], [16] or multipoint [14] driver models may not be required to capture driver steering behavior. Note that our measurements do *not* contradict empirical evidence that drivers use both a "near" and a "far" region of the visual field [6], on which the two-point steering models in [15], [16] are based. The driver's smoothing of the previewed target (characterized by $T_{l,f}$) requires that a substantial portion (or two distinct points) of the centerline is visible, while the generation of high-frequency lead ($T_{L,e^\star}$) may depend on observing optical flow patterns throughout the entire visual field [2], [4]. In other words, although drivers may rely on *multiple*, spatially separated optical cues for steering, their behavior can still be modeled using a *single* previewed target point as input. The proposed multiloop model further promises to provide understanding of driver control *adaptation* to task variables such as the vehicle dynamics, preview time, and road width and curvature, similar as provided by the crossover model for compensatory tracking tasks in the 1960s [20].

VII. Conclusions

This paper presented new human-in-the-loop experimental data, collected to improve our understanding of driver steering behavior on winding roads. For the very first time, three frequency-response function estimates of drivers' multiloop steering dynamics were obtained, providing unique evidence that drivers, besides lateral-position outer-loop control, rely on *heading feedback* to close a stabilizing inner-loop, and use preview of the centerline trajectory ahead for *feedforward* control. A multiloop, single preview-point driver model – directly extending the crossover model – captures this behavior. The proposed model's *physically interpretable* parameters provide unmatched understanding of, otherwise lumped, driver internal steering processes, quantifying the portion of the previewed centerline that is used for control, and how lateral position and heading feedback are weighed. The gained insights will potentially contribute to a better understanding of driver-automation interaction issues in modern road vehicles, and to the systematic design of *human-like* driver support systems.

References

[1] M. Sivak, "The information that drivers use: Is it indeed 90% visual?" *Perception*, vol. 25, no. 9, pp. 1081–1089, 1996.

[2] J. J. Gibson, "Visually controlled locomotion and visual orientation in animals," *Br. J. Psychol.*, vol. 49, no. 3, pp. 182–194, Aug. 1958.

[3] D. A. Gordon, "Perceptual basis of vehicular guidance: IV," *Public Roads*, vol. 34, no. 3, pp. 53–68, 1966.

[4] J. P. Wann and M. F. Land, "Steering with or without the flow: Is the retrieval of heading necessary?" *Trends in Cognitive Sciences*, vol. 4, no. 8, pp. 319–324, Aug. 2000.

[5] R. M. Wilkie and J. P. Wann, "Judgments of path, not heading, guide locomotion," *Journal of Experimental Psychology: Human Perception and Performance*, vol. 32, no. 1, pp. 88–96, Feb. 2006.

[6] M. F. Land and J. Horwood, "Which parts of the road guide steering?" *Nature*, vol. 377, pp. 339–340, Sep. 1995.

[7] I. Frissen and F. Mars, "The effect of visual degradation on anticipatory and compensatory steering control," *The Quarterly Journal of Experimental Psychology*, vol. 67, no. 3, pp. 499–507, 2014.

[8] O. Lappi, "Future path and tangent point models in the visual control of locomotion in curve driving," *Journal of Vision*, vol. 14, no. 12, pp. 1–22, Oct. 2014.

[9] D. T. McRuer, R. W. Allen, D. H. Weir, and R. H. Klein, "New results in driver steering control models," *Human Factors*, vol. 19, no. 4, pp. 381–397, Aug. 1977.

[10] E. Donges, "A two-level model of driver steering behavior," *Human Factors*, vol. 20, no. 6, pp. 691–707, Dec. 1978.

[11] R. A. Hess and A. Modjtahedzadeh, "A control theoretic model of driver steering behavior," *IEEE Control Systems Magazine*, vol. 10, no. 5, pp. 3–8, Aug. 1990.

[12] J. Steen, H. J. Damveld, R. Happee, M. M. van Paassen, and M. M., "A review of visual driver models for system identification purposes," in *IEEE Intern. Conf. on Sys., Man, and Cyb.*, 2011, pp. 2093–2100.

[13] K. van der El, D. M. Pool, and M. Mulder, "Measuring and modeling driver steering behavior: From compensatory tracking to curve driving," *Transportation Research Part F*, 2017.

[14] R. S. Sharp, D. Casanova, and P. Symonds, "A mathematical model for driver steering control, with design, tuning and performance results," *Vehicle System Dynamics*, vol. 33, no. 5, pp. 289 – 326, May 2000.

[15] D. D. Salvucci and R. Gray, "A two-point visual control model of steering," *Perception*, vol. 33, no. 10, pp. 1233–1248, Dec. 2004.

[16] L. Saleh, P. Chevrel, F. Claveau, J. F. Lafay, and M. F., "Shared steering control between a driver and an automation: Stability in the presence of driver behavior uncertainty," *IEEE Trans. on Intelligent Transportation Systems*, vol. 14, no. 2, pp. 974–983, Jun. 2013.

[17] D. H. Weir and D. T. McRuer, "Dynamics of driver vehicle steering control," *Automatica*, vol. 6, no. 1, pp. 87–98, Jan. 1970.

[18] D. T. McRuer, D. H. Weir, H. R. Jex, R. E. Magdaleno, and R. W. Allen, "Measurement of driver-vehicle multiloop response properties with a single disturbance input," *IEEE Transactions on Systems, Man, and Cybernetics*, vol. 5, no. 5, pp. 490–497, Sep. 1975.

[19] M. Mulder, D. M. Pool, D. A. Abbink, E. R. Boer, P. M. T. Zaal, F. M. Drop, K. van der El, and M. M. van Paassen, "Manual control cybernetics: State-of-the-art and current trends," *IEEE Trans. on Human-Machine Systems*, 2017.

[20] D. T. McRuer and H. R. Jex, "A review of quasi-linear pilot models," *IEEE Trans. on Human Factors in Electronics*, vol. 8, no. 3, pp. 231–249, May 1967.

[21] K. van der El, D. M. Pool, H. J. Damveld, M. M. van Paassen, and M. Mulder, "An empirical human controller model for preview tracking tasks," *IEEE Trans. on Cybernetics*, vol. 46, no. 11, pp. 2609–2621, Nov. 2016.

[22] K. van der El, D. M. Pool, M. M. van Paassen, and M. Mulder, "Effects of preview on human control behavior in tracking tasks with various controlled elements," *IEEE Trans. on Cybernetics*, vol. 48, no. 4, pp. 1242–1252, Apr. 2018.

[23] R. L. Stapleford, D. T. McRuer, and R. E. Magdaleno, "Pilot describing function measurements in a multiloop task," *IEEE Trans. on Human Factors in Electronics*, vol. 8, no. 2, pp. 113–125, Jun. 1967.

[24] H. J. Damveld, G. C. Beerens, M. M. van Paassen, and M. Mulder, "Design of forcing functions for the identification of human control behavior," *J. Guid. Control Dyn.*, vol. 33, no. 4, pp. 1064–1081, Jul. 2010.

[25] P. M. T. Zaal, D. M. Pool, J. de Bruin, M. Mulder, and M. M. van Paassen, "Use of pitch and heave motion cues in a pitch control task," *J. Guid. Control Dyn.*, vol. 32, no. 2, pp. 366–377, 2009.